Journal Pre-proofs

Non-amplified impedimetric genosensor for quantification of miRNA-21 based on the use of reduced graphene oxide modified with chitosan

Michael López Mujica, Yuanyuan Zhang, Fabiana Gutiérrez, Féthi Bédioui, Gustavo Rivas

Please cite this article as: M. López Mujica, Y. Zhang, F. Gutiérrez, F. Bédioui, G. Rivas, Non-amplified impedimetric genosensor for quantification of miRNA-21 based on the use of reduced graphene oxide modified with chitosan, *Microchemical Journal* (2020), doi: https://doi.org/10.1016/j.microc.2020.105596

Non-amplified impedimetric genosensor for quantification of miRNA-21 based on the use of reduced graphene oxide modified with chitosan

Michael López Mujica[1], Yuanyuan Zhang[2], Fabiana Gutiérrez[1,*], Féthi Bédioui[2,*], Gustavo Rivas[1,*]

[1]INFIQC-CONICET, Departamento de Fisicoquímica, Facultad de Ciencias Químicas, Universidad Nacional de Córdoba, Ciudad Universitaria. 5000 Córdoba, Argentina.

[2]Chimie ParisTech, PSL University, CNRS 2027, Institute of Chemistry for Life and Health Sciences, SEISAD 75005 Paris, France.

.

*Corresponding authors

*Email: fabigutierrez@gmail.com; fethi.bedioui@chimieparistech.psl.eu; grivas@fcq.edu.ar

Phone number: +54-351-5353866; Fax number: +54-351-4334188.

ABSTRACT

We report here an impedimetric genosensor for the quantification of microRNA-21 using $[Fe(CN)_6]^{3-/4-}$ as redox probe to transduce the hybridization event. The biosensing platform was built at a thiolated-gold electrode by covalent bond of reduced graphene oxide (RGO) modified with chitosan (CHIT) and further covalent attachment of the aminated DNA probe. GO was used to provide the carboxylic groups for the covalent attachment of CHIT and, once reduced, to improve the electroactivity of the resulting platform, while CHIT served as a bridge between the thiol and the aminated probe DNA. The proposed bioanalytical platform allows the label-free, non-amplified, simple and fast biosensing of microRNA-21, with a linear range between 1.0×10^{-12} M and 1.0×10^{-8} M, a sensitivity of (134 ± 4) ΩM^{-1} ($r^2 = 0.996$), a detection limit of 300 fM, and a reproducibility of 5.9 % for 1.0×10^{-12} M miRNA-21 and 2.2 % for 1.0×10^{-9} M miRNA-21. The genosensor was successfully used for the quantification of microRNA-21 in enriched human blood serum, urine and saliva samples.

Keywords: microRNA-21; Impedimetric biosensor; Biomarker; Graphene oxide; Chitosan.

1. Introduction

MicroRNAs (miRNAs) are non-coding RNAs of 19-25 nucleotides in length, that can be present in intergenic or intragenic regions of the genome and are involved in the post-transcriptional regulation of gene expression [1]. A dysregulation can be associated with cancer, dementia, and cardiovascular diseases, among other pathologies. miRNAs can have the role of tumor suppression or oncogenic function

and have been connected to with processes associated with cancer, such as apoptosis, invasion, metastasis, and proliferation [1]. Therefore, the development of highly sensitive and selective methodologies to quantify miRNAs, is highly required. Their low abundance, short length and high sequence-similarity with other family members, make the quantification of miRNAs a big challenge. In the last years there has been an increasing interest for the design of biosensors that allow the sensitive, selective and friendly quantification of miRNAs [2-4]. In this sense, the electrochemical ones have demonstrated to be very efficient [5].

miRNA-21 was one of the first mammalian miRNAs identified [6] and has been proposed as diagnostic and prognostic biomarker, and even as therapeutic target for several types of cancer [7]. The upregulation of miRNA-21 in breast, pancreatic, prostate, and colorectal cancers, makes a non-invasive diagnostic biomarker. Therefore, as it is upregulated in several types of cancer, is convenient to use miRNA-21 as part of a panel of biomarkers instead of a specific biomarker for one type of cancer [1].

Most of the electrochemical miRNA-21 biosensors reported in the last couple of years have been mainly based on the use of different amplification strategies. Zhang H. et al. [8] reported the use of a hairpin DNA modified-Au electrode associated with the action of a duplex specific nuclease (DSN), and the incorporation of a biotinylated signaling DNA/streptavidin-modified Au-nanoparticles(NPs)/biotinylated-horseradish peroxidase (HRP) to generate an enhanced analytical signal in the presence of hydrogen peroxide and 3,3,5,5´tetramethylbenzidine (TMB). A signal amplification mediated by PdNPs accumulated at a guanine-rich ssDNA generated through rolling circle amplification

3

(RCA) was also proposed [9]. Guo et al. [10] described the sub-fM biosensing by combination of a dual signal amplification strategy using hybridization chain reaction (HCR) and enzyme induced metallization (EIS). Tian et al. [11] described the use of a hairpin capture probe immobilized at Fe_3O_4, which is opened after interacting with miRNA-21, to allow the amplification by HCR and the synergized catalytic reduction of hydrogen peroxide/TMB system in the presence of a Cu(II) planar complex. Liang et al. [12] presented the pM detection of miRNA-21 using an amplification scheme based on HCR in connection with different strategies to transduce the hybridization event. An impedimetric quantification of miRNA-21, reported by Zhang et al. [13], was based on the use of glassy carbon electrode (GCE) modified with ZrO_2, graphene oxide (GO) and polyacrylic acid (PAA) containing the cyclically generated dsDNA from the hairpin unfolded after hybridization. The electrostatically accumulated $[Ru(NH)_6]^{3+}$ (RuHex) at different platforms following diverse schemes was used to generate the analytical signal either with or without the catalytic effect of $[Fe(CN)_6]^{3-}$ [14-16]. Feng et al. [17] proposed the voltammetric (SWV) quantification of miRNA-21 from the molybdophosphate generated through the facilitated accumulation of molybdate at the phosphate residues of the resulting DNA using HCR. Chen et al. [18] described a biosensor based on the SWV signal of the methylene blue (MB) released from mesoporous silica nanospheres-hairpin H1 and intercalated within the dsDNA generated at the gold electrode/capture DNA as a consequence of CHR after H1-miRNA-21 hybridization and CHA in the presence of the hairpin H2. A ratiometric scheme based on the different currents ratio of two redox markers before and after hybridization through mismatched catalytic hairpin assembly (CHA) amplification and generation of stable "Y"-shaped DNA complexes,

4

was reported by Li et al. [19]. Pingarrón´s group [20] reported an innovative alternative for the sub-pM detection of miRNA-21 using streptavidin-modified magnetic beads in connection with geno- and immunoassays and the detection at a magneto SPE through the use of anti DNA-RNA antibody modified with HRP. A highly sensitive DPV-detection of miRNA-21 through the sandwich hybridization with a thiolated capture probe-AuNPs-modified GCE and a MWCNTs-thionin-signaling probe, was also reported [21].

Although the non-amplified miRNA-21 electrochemical biosensors are not very frequent, some interesting alternatives have been also reported. Luo et al. [22] proposed the fM ratiometric detection of exosomal miRNA-21 using two redox markers located in a Y shape-like structure before and after hybridization. Ghazizadeh et al. [23] presented an original strategy by modifying SPE with MCF-exosomes and the protein p19. Kaugkamano et al. [24] described the fM detection of miRNA-21 through the decrease of Ag oxidation signal at Au modified with polypyrrol/Ag and pyrrolidinyl PNA. Bharti et al. [25] proposed the use of fluorine tin oxide (FTO) properly modified to support the biotinylated probe and the , with transduction of the hybridization event through the decrease of the DPV signal of $[Fe(CN)_6]^{3-/4-}$. The sub-pM detection of miRNA-21 based on the decrease of the SWV-thionin-redox signal at GCE/MoS$_2$-thionine-AuNPs was described by Zhu et al. [26]. Azzouzi et al. [27] proposed the impedimetric detection of miRNA-21 through the increment of the charge transfer resistance of a redox mediator produced by the anchoring of the complex biotin-molecular beacon-AuNPs-hybrid at the GCE/neutravidin.

5

The present work is focused on the development of a non-amplified impedimetric biosensor for miRNA-21 quantification taking advantage of the unique properties of graphenaceous materials in a double role of anchoring support to covalently immobilize the amine-rich polymer chitosan (CHIT) as graphene oxide (GO) and, as reduced graphene oxide (RGO), to improve to electroactivity of the resulting platform. The biosensing supramolecular architecture was built at 3-mercapto-1-propanesulfonate-modified gold electrode by self-assembling of RGO-CHIT and covalent attachment of NH_2-DNA probe. The transduction of the hybridization event was obtained from the change of the charge transfer resistance (R_{ct}) using $[Fe(CN)_6]^{3-/4-}$ as redox marker. In the following sections we discuss the characterization of the biosensing platform and the analytical performance of the resulting genosensor.

2. Experimental

2.1. Reagents

Sodium 3-mercapto-1-propanesulfonate (MPS), glutaraldehyde (glu), chitosan (CHIT), N-(3-dimethylaminopropyl)-N′-ethylcarbodiimide hydrochloride (EDC), N-hydroxy-succinimide (NHS), and bovin serum albumin (Alb) were purchased from Sigma. Potassium ferrocyanide was obtained from Merck and potassium ferricyanide from Biopack. Ethanol, sulfuric acid (98%) and sodium hydroxide were provided by J. T. Baker. Graphene oxide (GO, aqueous dispersion 4.0 mg mL^{-1}) was obtained from Graphenea. Other chemicals were reagent grade and used without further purification. DNA and RNA sequences, obtained from Invitrogen Life Technologies, are the following:

DNA probe: 5'-NH$_2$-TCA-ACA-TCA-GTC-TGA-TAA-GCT-A-3'

miRNA-21: 5'-UAG-CUU-AUC-AGA-CUG-AUG-UUG-A-3'

*Single-base mismatch: 5'-UAG-CUU-AUC-A**C**A-CUG-AUG-UUG-A-3'*

Non-complementary sequence: 5'-GGG-GGG-GGG-GGG-GGG-GGG-GGG-3'

Ultrapure water (ρ = 18.2 MΩ cm) from a Millipore-MilliQ system was used for preparing all the solutions.

2.2. Apparatus

A platinum wire and Ag/AgCl, 3 M NaCl (BAS) were used as counter and reference electrodes, respectively. All potentials are referred to the latter. The gold working electrodes were cleaned before each experiment by successive mechanical, chemical and electrochemical treatment. The mechanical treatment consisted in polishing with 0.05 µm alumina for 6 min, followed by sonication in deionized water for 5 min. Chemical treatment was performed by immersion in "Piranha" solution (1:3 v/v H_2O_2/H_2SO_4) for 5 min, followed by sonication for 10 seconds in ultrasonic bath and rinsing with ultrapure water. During the electrochemical treatment, the surfaces were stabilized in 0.500 M H_2SO_4 solution by applying two consecutives step potentials of 2.0 V and -1.0 V for 2 and 4 seconds, respectively. The state of the surface after the pretreatment was evaluated by cyclic voltammetry at 0.100 Vs^{-1} in a 0.500 M H_2SO_4 solution.

Electrochemical Impedance Spectroscopy (EIS) measurements were performed with a PGSTAT30 potentiostat (Methrom). The redox probes were 1.0 x 10^{-3} M [Fe(CN)$_6$]$^{3-}$/[Fe(CN)$_6$]$^{4-}$ and the experiments were carried out in a 0.050 M

phosphate buffer solution pH 7.40. EIS parameters were the following, amplitude: 0.010 V, frequency range: between 1.0×10^{-2} and 1.0×10^{6} Hz, and working potential: 0.200 V. The impedance spectra were analyzed and fitted by using the Z-view program.

UV-Vis experiments were carried out with a Shimadzu UV1601 spectrophotometer and a quartz cuvette of 0.1 cm path length.

2.3. Synthesis of RGO-CHIT

A volume of 3.125 mL of 4.0 mgmL^{-1} GO solution was mixed with 6.875 mL of a 2.00 mgmL^{-1} CHIT solution previously prepared in a 0.100 M 2-(N-morpholino)ethanesulfonic acid (MES) pH 5.00 by sonicating for 2 h in ultrasonic bath. The resulting GO-CHIT mixture was sonicated in ultrasonic bath for 2 h to obtain a homogeneous dispersion. After that, the carboxylate groups of GO were activated with 0.100 M EDC and 0.100 M NHS by sonication for 2 hours and overnight reaction until completeness under stirring conditions. The purification of GO-CHIT was carried out by centrifugation for 60 min at 3500 rpm and further resuspension of the pellet in a 0.15 M MES buffer pH 5.00. This process was repeated 4 times to eliminate the excess of CHIT. Subsequently, RGO-CHIT was chemically reduced by adding excess of NaBH$_4$ and stirring for 24 h. The resulting RGO-CHIT was washed following the same procedure as indicated before for washing GO-CHIT. The characterization of the synthesis was carried out by UV-vis spectroscopy, following the displacement of the GO extinction band at 234 nm (Figure 1-SI).

2.4. Construction of the biosensing platform

Figure 1 presents a schematic illustration of the different steps followed during the construction of the biosensing platform. The gold electrode was modified with a 2.00×10^{-2} M MPS solution (prepared in 1.60×10^{-3} M H_2SO_4) for 60 min. After washing the surface with the sulphuric acid solution and water, RGO-CHIT was electrostatically adsorbed for 60 min. Once the RGO-CHIT was immobilized at the electrode surface and after washing with MES, the amine residues were activated with 1.0 % v/v glutaraldehyde (prepared in 1% v/v CH_3COOH). Previous washing of the surface with 0.050 M phosphate buffer solution pH 7.40, the probe was covalently attached by depositing 20 μL of 50 ppm NH_2-DNA probe solution (prepared in 0.050 M phosphate buffer pH 7.40 + 0.500 M NaCl) at the electrode surface for 30 min. After this step, the surface was washed with 0.050 M phosphate buffer pH 7.40 + 0.500 M NaCl and before performing the hybridization, the surface was blocked with 2.0 % w/v albumin for 30 min to avoid non-specific adsorptions. The hybridization was performed at the resulting Au/MPS/RGO-CHIT/DNA$_{probe}$ biosensing platform by dropping the 20 μL of miRNA-21 solution (prepared in 0.050 M phosphate buffer solution pH 7.40 + 0.500 M NaCl) for 75 min.

3. Results and discussion

Figure 2A shows the Nyquist plots obtained after each step during the construction of the biosensing supramolecular arquitecture (Au, Au/MPS, Au/MPS/RGO-CHIT, Au/MPS/RGO-CHIT/DNA$_{probe}$, Au/MPS/RGO-CHIT/DNA$_{probe}$/Alb) and after the hybridization event (Au/MPS/RGO-CHIT/DNA$_{probe}$/miRNA-21) using 1.0×10^{-3} M $[Fe(CN)_6]^{3-}$/$[Fe(CN)_6]^{4-}$ as redox

9

probe. The circles correspond to the experimental points while the solid lines represent the fitting with the model, in this case a Randles circuit, where R_s is the solution resistance, R_{ct} is the charge transfer resistance, C_{dl} the capacitance of the double-layer and W, the Warburg impedance (Inset of Figure 2A). Figure 2B depicts the variation of R_{ct} obtained from the Nyquist plots shown in Figure 2A. The attachment of MPS at Au produced the expected increment of R_{ct} due to the blocking effect of the thiol and the electrostatic repulsion with the redox marker. The adsorption of RGO-CHIT does not produce a significant change in R_{ct} due to the compensation of different effects: the facilitated electrostatic interaction between CHIT and $[Fe(CN)_6]^{3-}/[Fe(CN)_6]^{4-}$ and the conductive nature of RGO that would facilitate the charge transfer, and the blocking effect of CHIT that would make more difficult the charge transfer of the redox probe. Once the DNA probe is immobilized at Au/MPS/RGO-CHIT, R_{ct} increases due to the blocking effect of the non-conductive nucleic acid layer and the electrostatic repulsion of the redox marker with the negatively charge ribose-phosphate backbone of DNA. The incorporation of Alb, to avoid the non-specific adsorption, produces a small decrease of R_{ct} mainly due to the shielding of the negative charges of DNA probe that compensates the blocking effect of the non-conductive protein. Once the hybridization with 1.0×10^{-8} M miRNA-21 takes place, there is an important increment of R_{ct} due to the increase of the electrostatic repulsion between the redox probe and the higher negative charge density as a consequence of the surface heteroduplex formation.

The effect of the hybridization time was evaluated from similar experiments performed with 1.0×10^{-9} M miRNA-21. There was an increment in the R_{ct} with the hybridization time from 30 to 75 min mainly due to the increase of the electrostatic

10

repulsion between the redox marker and the enhanced negative charge density resulting from the formation of a higher amount of DNA-miRNA-21 with the hybridization time, to slightly decrease thereafter (Figure 2-SI). We selected 75 min as the best compromise between sensitivity, reproducibility and assay time.

Figure 3A depicts the Nyquist plots obtained for Au/MPS/RGO-CHIT/DNA/Alb in the presence of different concentrations of miRNA-21 from 1.0×10^{-12} M to 1.0×10^{-8} M, and Figure 3B shows the plot of the corresponding R_{ct} as a function of miRNA-21 concentration. There is a linear dependence in the whole range between 1.0×10^{-12} M and 1.0×10^{-8} M miRNA-21, with a sensitivity of (134 ± 4) ΩM^{-1} ($r^2 = 0.996$) and a detection limit of 300 fM (calculated as 3 x SD/s where SD is the standard deviation of the blank signal and s, the sensitivity). The reproducibility, obtained from the determination of 1.0×10^{-12} M miRNA-21 was 5.9 % while for 1.0×10^{-9} M miRNA-21, it was 2.2 %.

Figure 4 shows the bars plot for the R_{ct} of the redox marker obtained at Au/MPS/RGO-CHIT/DNA$_{probe}$/Alb in the presence of 1.0×10^{-9} M miRNA-21, one-base mismatch sequence and a fully non-complementary sequence, to evaluate the selectivity of the genosensor. No response was observed in the case of the fully non-complementary sequence compared to the blank while for the one-base mismatch sequence, the R_{ct} is only 24.2 % of the complementary one, clearly indicating that the genosensor is able to discriminate non-complementary and even one-base mismatch sequences.

Considering that miRNA-21 can be found in different biological fluids and that, depending on the nature of the cancer, it is relevant to use one or other fluid, we evaluate the usefulness of our biosensor to quantify miRNA-21 in: saliva, urine and

11

reconstituted human serum samples diluted (1:10 (saliva and urine) and 1:1000 (serum samples)), with 0.050 M phosphate buffer solution pH 7.40 + 0.500 M NaCl) and enriched with 1.0 x 10^{-9} M miRNA-21. The recovery values were (96 ± 3) %, (90 ± 2) %, and (98 ± 3) % for urine, saliva and serum, respectively. It is important that analogue experiments performed with the diluted samples without miRNA-21, did not show any matrix effect, with interferences in R_{ct} of 1.9%, 2.3 % and 1,0 % for reconstituted serum, urine and saliva, respectively. These results indicate that the proposed genosensor can be successfully used for practical applications in different biological fluids.

Table 1 compares the analytical performance of our biosensor with the most relevant miRNA-21 electrochemical biosensors reported in the last couple of years. Among them, most of the electrochemical biosensors based on the use of amplification schemes detection limits (femtomolar to attomolar) than our biosensor (300 fM) [8-11, 13-19, 25] while few of the amplified biosensors present higher detection limits than the proposed biosensing platform [12, 20]. Regarding the non-amplified detection, our biosensor presents better detection limits than the strategies reported in references [26, 27] and higher than those described in references [23, 24]. In summary, even when our biosensor does not present better detection limits than most of the biosensors reported in the Table 1, it is still competitive since it is possible to quantify miRNA-21 even at fM levels in a simple and fast way, without using amplification strategies involving labelling enzymes/redox markers, endonucleases, special isothermal amplification schemes, different nanomaterials, oligonucleotides with particular structures, and DNA analogues [8-11, 13-19, 25] or

non-amplified strategies based on the use of expensive noble metal nanoparticles [21, 24, 25].

4. CONCLUSIONS

This work reported an original, label-free and non-amplified impedimetric genosensor for miRNA-21 using a bioanalytical platform rationally built by taking advantage of the carboxylic groups of GO to support CHIT, the conductive properties of RGO to improve the electroactivity of the platform, and the high density of the amine groups of chitosan to work as bridge between MPS and the aminated capture probe. The resulting genosensor allowed the sensitive (femtomolar), selective, simple and fast quantification of miRNA-21 without any additional amplification step and successful application in different biological fluids.

In addition to these advantages for the quantification of miRNA-21, that make Au/MPS/RGO-CHIT/DNA competitive, it is a versatile bioanalytical platform that opens new horizons for multiple biosensing applications just selecting the most appropriate biorecognition element.

ACKNOWLEDGEMENTS

DECLARATION OF CONFLICT OF INTEREST

No authors have any conflicts of interest to disclose.

REFERENCES

1. D. Bautista-Sánchez, C. Arriaga-Canon, A. Pedroza-Torres, A. De La Rosa-Velázquez, R. González-Barrios, L. Contreras-Espinosa, R. Montiel-Manríquez, C. Castro-Hernández, V. Fragoso-Ontiveros, R. María Álvarez-Gómez, L.A. Herrera, The Promising Role of miR-21 as a Cancer Biomarker and Its Importance in RNA-Based Therapeutics, Molec. Ther.: Nuc. Aci. 20 (2020) 409-420.

2. M.K. Masud, M. Umer, M.S.A. Hossain, Y. Yamauchi, N.T. Nguyen, M.J.A. Shiddiky, Nanoarchitecture Frameworks for Electrochemical miRNA Detection, Trends Biochem. Sci. 44 (2019) 433-452.

3. P. Gillespie, S. Ladame, D. O'Hare, Molecular methods in electrochemical microRNA detection, Analyst 144 (2019) 114-129.

4. M. López Mujica, Y. Zhang, F. Bédioui, F. Gutiérrez, G. Rivas, Label-free graphene oxide–based SPR genosensor for the quantification of microRNA21, Anal. Bioanal. Chem. 412 (2020) 3539–3546.

5. H. Mohammadi, G. Yammouri, A. Amine, Current advances in electrochemical genosensors for detecting microRNA cancer markers, Curr. Opin. Electroche. 16 (2019) 96-105.

6. M. Lagos-Quintana, R. Rauhut, W. Lendeckel, T. Tuschl, Identification of novel genes coding for small expressed RNAs, Science 294 (2001) 853-858.

7. R. Rupaimoole, F. Slack, MicroRNA therapeutics: towards a new era for the management of cancer and other diseases, Nat. Rev. Drug Discov. 6 (2017) 203–222.

8. H. Zhang, M. Fan, J. Jiang, Q. Shen, C. Cai, J. Shen, Sensitive electrochemical biosensor for MicroRNAs based on duplex-specific nuclease-assisted target recycling followed with gold nanoparticles and enzymatic signal amplification, Anal. Chim. Acta. 1064 (2019) 33-39.

9. C. Zhang, D. Li, D. Li, K. Wen, X. Yang, Y. Zhu, Rolling circle amplification-mediated: In situ synthesis of palladium nanoparticles for the ultrasensitive electrochemical detection of microRNA, Analyst 144 (12) (2019) 3817-3825.

10. W.J. Guo, Z. Wu, X.Y. Yang, D.W. Pang, Z.L. Zhang, Ultrasensitive electrochemical detection of microRNA-21 with wide linear dynamic range based on dual signal amplification, Biosens. Bioelectron. 131 (2019) 267-273.

11. L. Tian, J. Qi, O. Oderinde, C. Yao, W. Song, Y. Wang, Planar intercalated copper (II) complex molecule as small molecule enzyme mimic combined with Fe_3O_4 nanozyme for bienzyme synergistic catalysis applied to the microRNA biosensor, Biosens. Bioelectron. 110 (2018) 110-117.

12. M. Liang, M. Pan, J. Hu, F. Wang, X. Liu, Electrochemical Biosensor for MicroRNA Detection Based on Cascade Hybridization Chain Reaction, ChemElectroChem. 5 (2018) 1380-1386.

13. K. Zhang, N. Zhang, L. Zhang, H. Wang, H. Shi, Q Liu, Label-free impedimetric sensing platform for microRNA-21 based on ZrO_2-reduced graphene oxide nanohybrids coupled with catalytic hairpin assembly amplification, RSC Adv. 8 (2018) 16146-16151.

14. B. Bo, T. Zhang, Y. Jiang, H. Cui, P. Miao, Triple Signal Amplification Strategy for Ultrasensitive Determination of miRNA Based on Duplex Specific Nuclease and Bridge DNA-Gold Nanoparticles, Anal. Chem. 20 (2018) 2395-2400.

15. A. Ganguly, J. Benson, P. Papakonstantinou, Sensitive chronocoulometric detection of miRNA at screen-printed electrodes modified by gold-decorated MoS_2 nanosheets, ACS Appl. Bio Mater. 1 (2018) 1184-1194.

16. M.N. Islam, L. Gorgannezhad, M.K. Masud, S. Tanaka, M.S.A. Hossain, Y. Yamauchi, N.T. Nguyen, M.A. Shiddiky, Graphene-Oxide-Loaded Superparamagnetic Iron Oxide Nanoparticles for Ultrasensitive Electrocatalytic Detection of MicroRNA, ChemElectroChem. 5 (2018) 2488-2495.

17. K. Feng, J. Liu, L. Deng, H. Yu, M. Yang, Amperometric detection of microRNA based on DNA-controlled current of a molybdophosphate redox probe and amplification via hybridization chain reaction, Microchim. Acta 185 (2018) 185:28.

18. H. Cheng, W. Li, S. Duan, J. Peng, J. Liu, W. Ma, H. Wang, X. He, K. Wang, Mesoporous Silica Containers and Programmed Catalytic Hairpin Assembly/Hybridization Chain Reaction Based Electrochemical Sensing Platform for MicroRNA Ultrasensitive Detection with Low Background, Anal. Chem. 91 (2019) 10672-10678.

19. X. Li, B. Dou, R. Yuan, Y. Xiang, Mismatched catalytic hairpin assembly and ratiometric strategy for highly sensitive electrochemical detection of microRNA from tumor cells, Sensor Actuat. B-Chem. 286 (2019) 191-197.

20. E. Vargas, R.M. Torrente-Rodríguez, V.R.V. Montiel, E. Povedano, M. Pedrero, J.J. Montoya, S. Campuzano, J.M. Pingarrón, Magnetic beads-based sensor with tailored sensitivity for rapid and single-step amperometric determination of miRNAs, Int. J. Mol. Sci. 18 (2017) 2151.

21. K. Deng, X. Liu, C. Li, H. Huang, Sensitive electrochemical sensing platform for microRNAs detection based on shortened multi-walled carbon nanotubes with high-loaded thionin, Biosens. Bioelectron. 117 (2018) 168-174.

22. L. Luo, L. Wang, L. Zeng, Y. Wang, Y. Weng, Y. Liao, T. Chen, Y. Xia, J. Zhang, J. Chen, A ratiometric electrochemical DNA biosensor for detection of exosomal MicroRNA, Talanta 207 (2020) 120298.

23. E. Ghazizadeh, Z. Naseri, M.R. Jaafari, M. Forozandeh-Moghadam, S. Hosseinkhani, A fires novel report of exosomal electrochemical sensor for sensing micro RNAs by using multi covalent attachment p19 with high sensitivity, Biosens. Bioelectron. 113 (2018) 74-81.

24. T. Kangkamano, A. Numnuam, W. Limbut, P. Kanatharana, T. Vilaivan, P. Thavarungkul, Pyrrolidinyl PNA polypyrrole/silver nanofoam electrode as a novel label-free electrochemical miRNA-21 biosensor, Biosens. Bioelectron. 102 (2018) 217-225.

25. A. Bharti, N. Agnihotri, N. Prabhakar, A voltammetric hybridization assay for microRNA-21 using carboxylated graphene oxide decorated with gold-platinum bimetallic nanoparticles, Microchim. Acta 186 (2019) 185.

26. D. Zhu, W. Liu, D. Zhao, Q. Hao, J. Li, J. Huang, J. Shi, J. Chao, S. Su, L. Wang, Label-Free Electrochemical Sensing Platform for MicroRNA-21

Detection Using Thionine and Gold Nanoparticles Co-Functionalized MoS_2 Nanosheet, ACS Appl. Mater. Inter. 9 (2017) 35597-35603.

27. S. Azzouzi, W.C. Mak, K. Kor, A.P.F. Turner, M.B. Ali, V. Beni V, An integrated dual functional recognition/amplification bio-label for the one-step impedimetric detection of Micro-RNA-21, Biosens. Bioelectron. 92 (2017) 154-161.

LEGENDS OF THE FIGURES

Figure 1. Schematic representation of the different steps during the building of the miRNA-21 genosensor.

Figure 2. (**A**) Nyquist plots obtained during the construction of biosensor. Inset: Equivalent circuit used to fit the experimental results (**B**) Charge transfer resistance after each step during the construction of the biosensing layer and after the hybridization with 1.0×10^{-8} M miRNA-21. Redox marker: 1.0×10^{-3} M $[Fe(CN)_6]^{3-}/[Fe(CN)_6]^{4-}$; Frequency range: 10 KHz to 10 mHz; Potential amplitude: 10 mV; Working potential: 0.200 V. Supporting electrolyte: 0.050 M phosphate buffer solution pH 7.40 with 0.500 M NaCl.

Figure 3. (**A**) Nyquist plots for 1.0×10^{-3} M $[Fe(CN)_6]^{3-}/[Fe(CN)_6]^{4-}$ obtained at Au/MPS/RGO-CHIT/DNA$_{probe}$ for different concentrations of miRNA-21. Redox marker: 1.0×10^{-3} M $[Fe(CN)_6]^{3-}/[Fe(CN)_6]^{4-}$. Other conditions as in Figure 2.

Figure 4. Charge transfer resistances obtained at GCE/MPS/RGO-CHIT/DNA in the presence of 1.0×10^{-9} M miRNA-21, 1-base-missmatch, and fully non-complementary sequences. Hybridization time: 75 min. Other conditions as in Figure 2.

Table 1. Comparison of the analytical parameters for the most relevant miRNA-21 electrochemical biosensors reported in the last two years.

Figure 1-SI. UV-vis spectra corresponding to GO-CHIT (**-**) and RGO-CHIT (**-**)

Figure 2-SI. Effect of the hybridization time at Au/MPS/RGO-CHIT/DNA/Alb on the R_{ct} in the presence of 50 ppm NH_2-DNA. Concentration miRNA-21: 1 x 10^{-9} M. Redox marker: 1.0 x 10^{-3} M $[Fe(CN)_6]^{3-}/[Fe(CN)_6]^{4-}$; Frequency range: 10 KHz to 10 mHz; Potential amplitude: 10 mV; Working potential: 0.200 V. Supporting electrolyte: 0.050 M phosphate buffer solution pH = 7.40 with 0.500 M NaCl.

AUTHORSHIP STATEMENT

Manuscript title: __" **Non-amplified impedimetric genosensor for quantification of miRNA-21 based on the use of reduced graphene oxide modified with chitosan"**

All persons who meet authorship criteria are listed as authors, and all authors certify that they have participated sufficiently in the work to take public responsibility for the content, including participation in the concept, design, analysis, writing, or revision of the manuscript. Furthermore, each author certifies that this material or similar material has not been and will not be submitted to or published in any other publication before its appearance in the Hong Kong Journal of Occupational Therapy.

Authorship contributions

Please indicate the specific contributions made by each author (list the authors' initials followed by their surnames, e.g., Y.L. Cheung). The name of each author must appear at least once in each of the three categories below.

Category 1

Conception and design of study: _RIVAS GUSTAVO, FETHI BEDIOUI
Acquisition of data: ___MICHAEL LÓPEZ MUJICA; YUANYUAN ZHANG

Analysis and/or interpretation of data: FABIANA GUTIERREZ, FETHI BEDIOUI, GUSTAVO RIVAS

Category 2
Drafting the manuscript: _____RIVAS GUSTAVO, FETHI BEDIOUI
Revising the manuscript critically for important intellectual content: RIVAS GUSTAVO, FETHI BEDIOUI
Category 3
Approval of the version of the manuscript to be published (the names of all authors must be listed): MICHAEL LÓPEZ MUJICA, YUANYUAN ZHANG, FABIANA GUTIERREZ, FETHI BEDIOUI, GUSTAVO RIVAS.
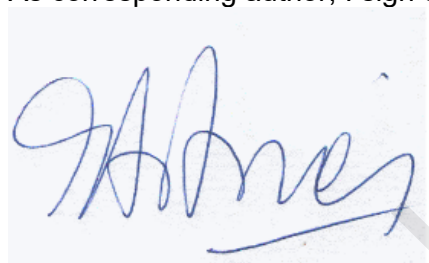**Acknowledgements**
All persons who have made substantial contributions to the work reported in the manuscript (e.g., technical help, writing and editing assistance, general support), but who do not meet the criteria for authorship, are named in the Acknowledgements and have given us their written permission to be named. If we have not included an Acknowledgements, then that indicates that we have not received substantial contributions from non-authors. This statement is signed by all the authors (a photocopy of this form may be used if there are more than 10 authors):
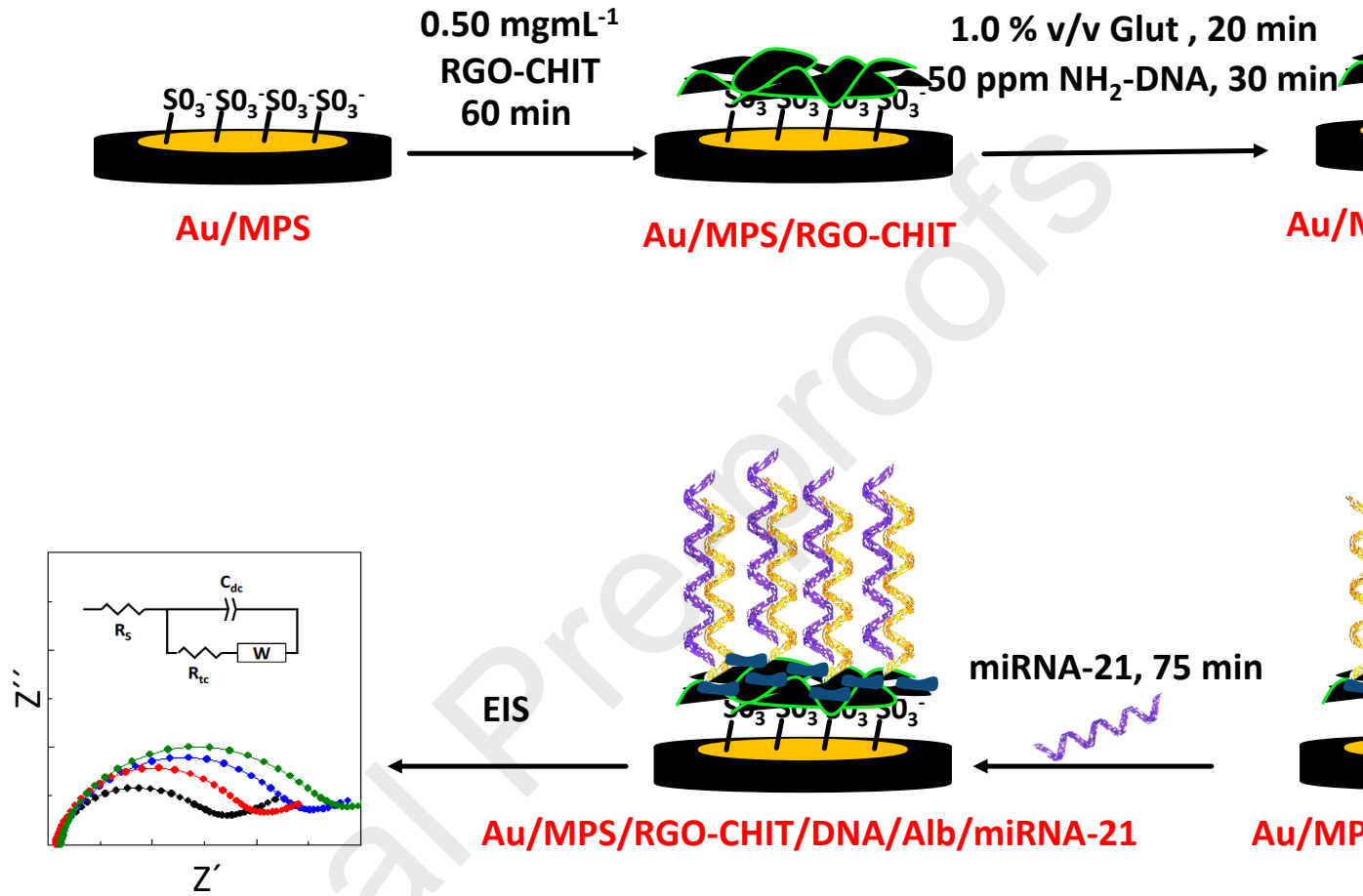Author's name (typed) Author's signature Date
August 31, 2020_____ _____ _____
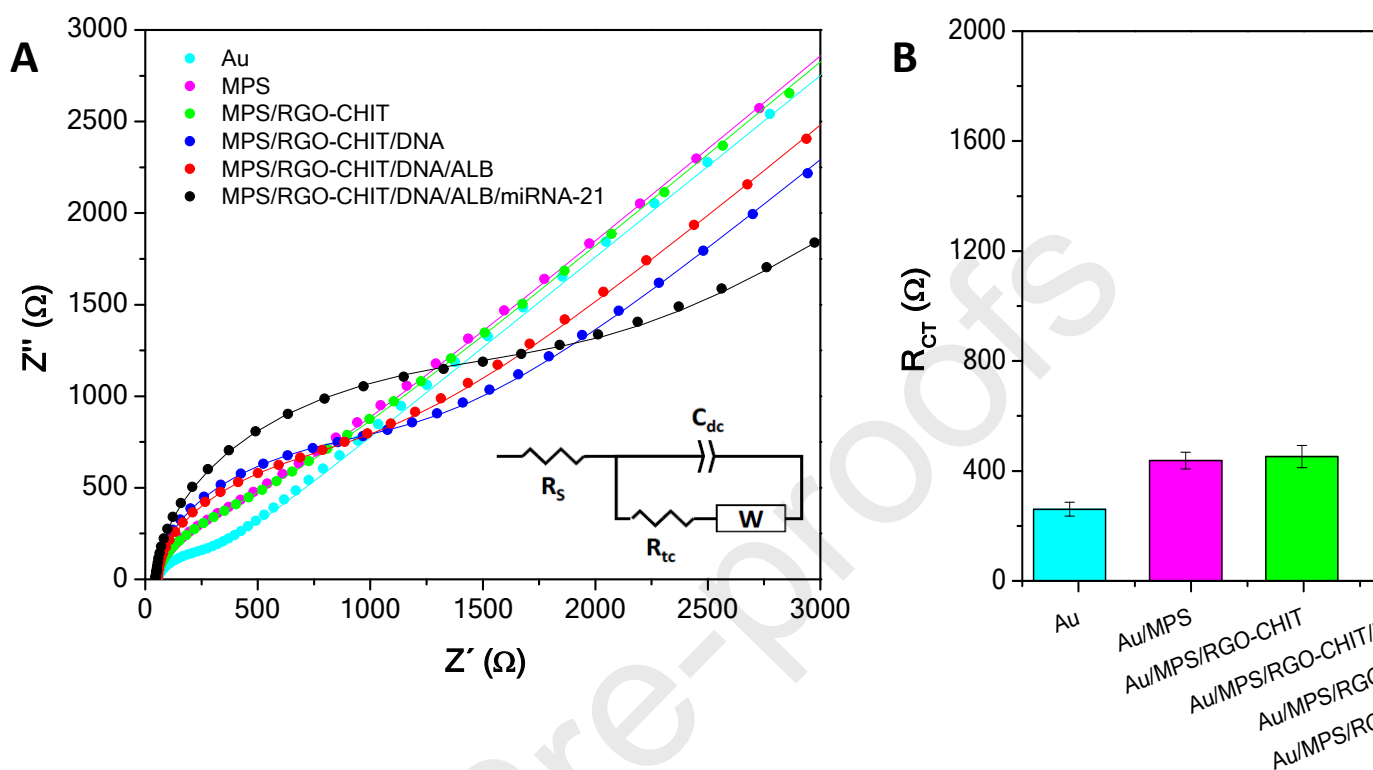As corresponding author, I sign on behalf of all the authors

GUSTAVO RIVAS

The authors of the manuscript "**Non-amplified impedimetric genosensor for quantification of miRNA-21 based on the use of reduced graphene oxide modified with chitosan"**, Michael López Mujica, Yuanyuan Zhang, Fabiana Gutierrez, Fethi Bedioui and Gustavo Rivas declare that there are no conflicts of interest.

0.50 mgmL^{-1}
RGO-CHIT
60 min

1.0 % v/v Glut , 20 min
50 ppm NH$_2$-DNA, 30 min

SO$_3^-$ SO$_3^-$ SO$_3^-$ SO$_3^-$

SO$_3^-$ SO$_3^-$ SO$_3^-$ SO$_3^-$

Au/MPS

Au/MPS/RGO-CHIT

Au/M

C$_{dc}$

R$_S$

R$_{tc}$ W

Z′′

Z′

EIS

miRNA-21, 75 min

SO$_3^-$ SO$_3^-$ SO$_3^-$ SO$_3^-$

Au/MPS/RGO-CHIT/DNA/Alb/miRNA-21

Au/MP

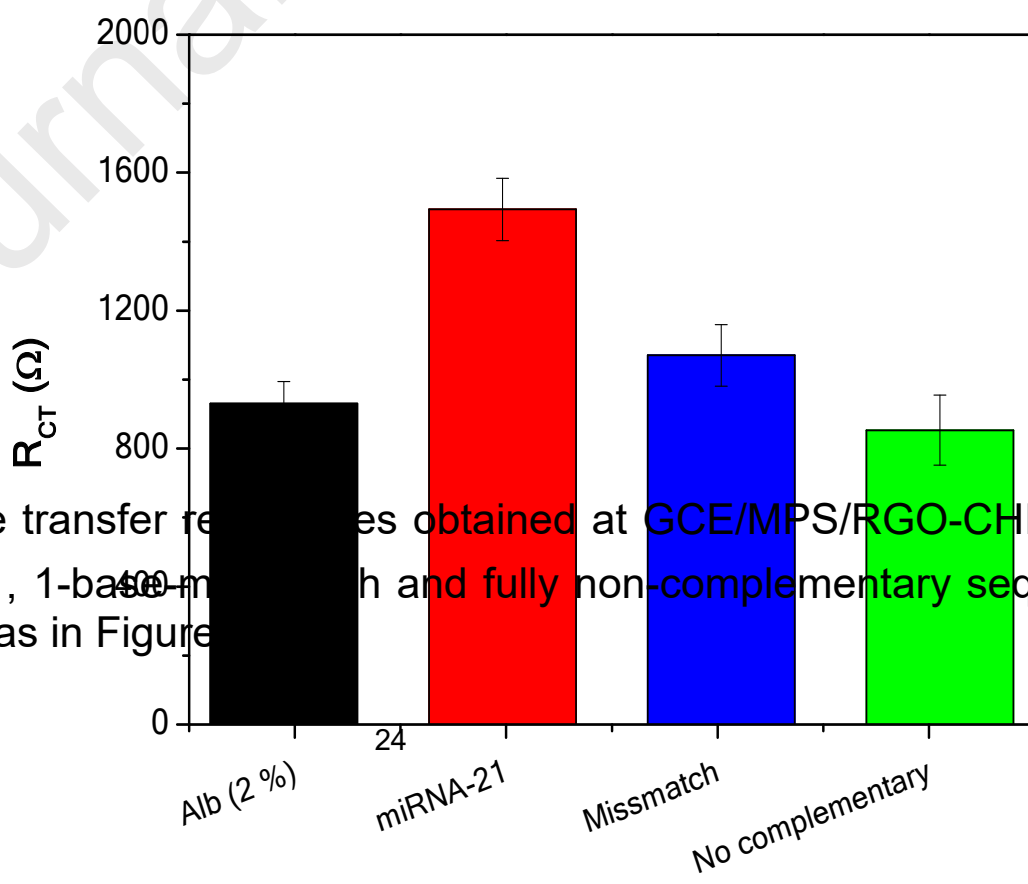**Figure 1**. Different steps during the building of the miRNA-21

Figure 2. (**A**) Nyquist plots obtained during the construction of biosensor. Inse
to fit the experimental results (**B**) Charge transfer resistance after each step o
the biosensing layer and after the hybridization with 1.0×10^{-8} M miRNA-21. F
M $[Fe(CN)_6]^{3-}/[Fe(CN)_6]^{4-}$; Frequency range: 10 KHz to 10 mHz; Potential am
potential: 0.200 V. Supporting electrolyte: 0.050 M phosphate buffer solutio
NaCl.

23
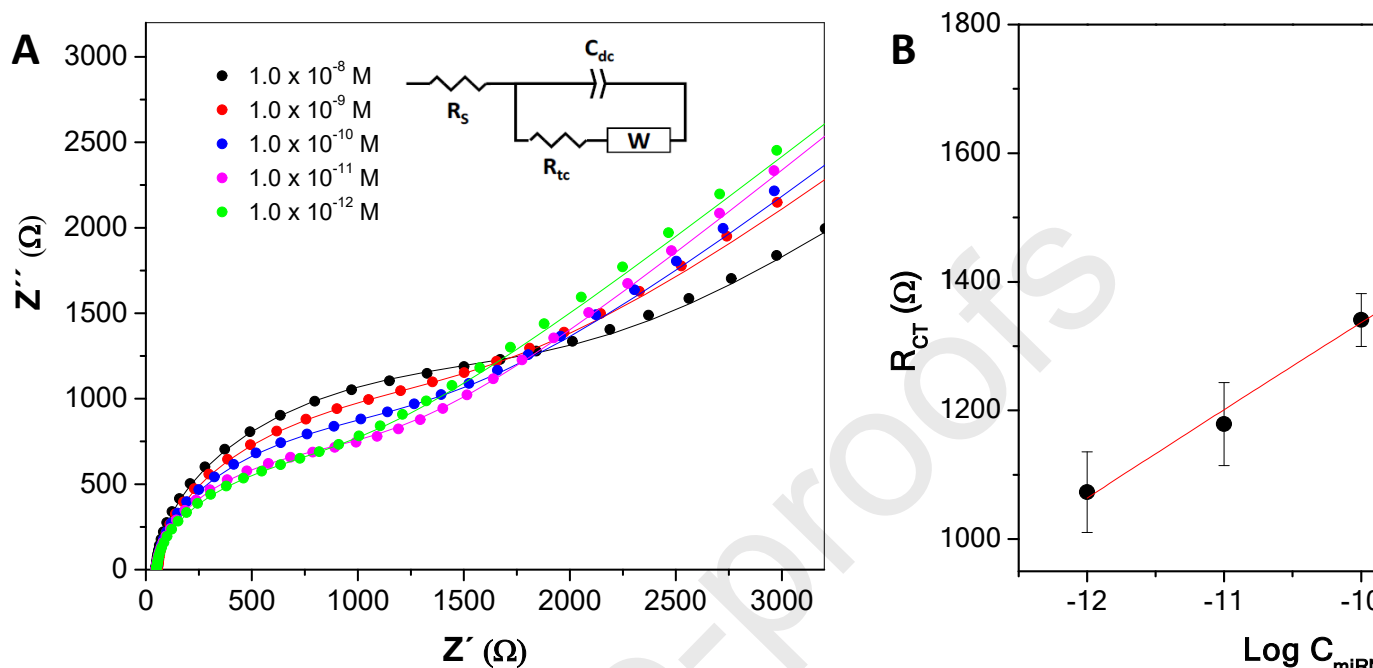
Figure 3. (**A**) Nyquist plots for 1.0 x 10^{-3} M [Fe(CN)$_6$]$^{3-}$/[Fe(CN)$_6$]$^{4-}$ obtained at different concentrations of miRNA-21. Redox marker: 1.0 x 10^{-3} M [Fe(CN)$_6$]$^{3-}$/[as in Figure 2.

Figure 4. Charge transfer re es obtained at GCE/MPS/RGO-CHIT/Alb/DN 10^{-9} M miRNA-21, 1-base-m h and fully non-complementary sequences. Other conditions as in Figure

24

...que	Electrode	Platform and detection	DL	LR	Real sample
...ometry	Au	Hairpin DNA modified-gold electrode, DSN-assisted target recycling, biotinylated signaling DNA/streptavidin-AuNPs to anchor the biotinylated HRP.	43 aM	0.1 fM to 100 pM	Tumor cells
	Au	G-rich long ssDNAs generated by RCA to facilitate the *in situ* synthesis of PdNPs .	8.6 aM	50 aM to 100 fM	Human serum
	Au	Integration of a dual signal amplification strategy of HCR and EIM, using capture probe (CP H1) modified magnetic nanobeads.	0.84 fM	1.0×10^{-15} M to 1.0×10^{-8} M	Human serum
	MGCE	Capture hairpin immobilized at Fe_3O_4, amplification using HCR and detection from the synergistic reduction of hydrogen peroxide/ TMB system in the presence of a Cu(II) planar complex.	33 aM	100 aM to 100 nM	Human serum
	Au	Amplification scheme based on HCR, which leads to extended growth of DNA chains and higher amplification efficiency through MB intercalation.	11 pM	30 pM to 7.0 nM	Human serum
	GCE	ZrO_2/rGO/modified electrode coupled with CHA signal amplification strategy and detection through the change of charge transfer resistance of $[Fe(CN)_6]^{3-/4-}$.	4.3×10^{-15} M	1.0×10^{-14} M to 1.0×10^{-10} M	MCF7 cells and human embryonic kidney cells
...coulometry	Au	Triple signal amplification based on target-triggered cyclic duplex specific nuclease digestion and bridge DNA/AuNPs; detection from the preconcentrated $[Ru(NH_3)_6]^{3+}$.	6.8 aM	1.0×10^{-17} M to 1.0×10^{-11} M	Human serum
...coulometry	SPE	MoS_2@AuNPs/capture DNA and detection through the $[Ru(NH_3)_6]^{3+}$ electrostatically bond to the surface hybrid.	100 aM	10 fM to 10 pM	-
...coulometry	SPCE	GO-loaded iron oxide and detection from $[Ru(NH_3)_6]^{3+}$ catalyzed by $[Fe(CN)_6]^{3-}$.	1.0 fM	1.0 fM to 1.0 nM	Ovarian cancer and normal non-cancerous cells
	Au	Thiol-modified hairpin capture probe immobilized at Au, detection carried out through the molybdophosphate accumulated at the ribose-phosphate backbone of the resulting duplex.	0.5 fM	1.0 fM to 1.0 nM	Human serum
	Au	Mesoporous silica nanospheres-hairpin H1, CHA and HCR enzyme-free amplification, and detection from the nanospheres-released MB.	0.037 fM	0.1 fM to 5.0 pM	Liver hepatocellular cells
	Au	Ratiometric scheme based on target driven CHA mismatched using three hairpins. Detection from the currents ratio of two redox markers before and after hybridization.	1.1 fM	5.0 fM to 0.1 nM	Cell extraction samples from the MCF7
...ometry	SPCE	Geno- and immunoassay using anti DNA-RNA antibody and detection from the bacterial protein A conjugated with poly-HRP40/hydrogen peroxide.	0.4 pM	1.0 pM to 100 pM	Cancer cells and tumor tissues
	GCE	DNA-AuNPs, miRNA-21 and MWCNTs modified with a signaling DNA and labeled with thionine.	0.032 pM	0.1 pM to 12000 pM	-
	GCE	LNA-modified "Y" shape-like structure and detection of exosomal miRNA-21 based on the	2.3 fM	10 fM-70 fM	Exosomes samples

	distance-sensitive currents ratio of two redox markers.			
SPE	Immobilized p19 protein with MCF-exosome biomarkers and subsequent detection due activation of the system by target addition.	1.0 aM	1.0 pM to 100 nm	-
Au	Electrode modified with polypyrrol/Ag and pyrrolidinyl PNA and detection through the decrease of Ag oxidation signal.	10 fM	1.0×10^{-13} M to 1.0×10^{-8} M	Human plasma
FTO	CGO/Au-PtBNPs/SA/CP using $[Fe(CN)_6]^{3-/4}$ as redox probe.	1.0 fM	1.0 fM to 1.0 µM	Human serum
GCE	MoS$_2$-Thi-AuNPs nanohybrid as a signaling molecule to monitor DNA-RNA hybridization. Detection from the decrease in the electrochemical signal of Thi.	0.26 pM	1.0 pM to 10 nM	Human serum
GCE	Neutravidin and a highly specific biotinylated DNA/LNA molecular beacon probe conjugated with AuNPs and detection by increment of the charge transfer resistance of a redox probe	0.3 pM	1.0 pM to 1000 pM	Human serum

DL: detection limit; LR: linear range; DSN: duplex-specific nuclease; AuNPs: gold nanoparticles; HRP: horseradish peroxidase; DPV: differential pulse voltammetry; ssDNA: single-stranded DNA; RCA: rolling circle amplification; PdNPs: palladium nanoparticles; HCR: hybridization chain reaction; EIM: enzyme-induced metallization; MGCE: magnetic glassy carbon electrode; TMB: 3,3',5,5'-tetramethylbenzidine; MB: methylene blue; EIS: electrochemical impedance spectroscopy; GCE: glassy carbon electrodes; rGO: reduced graphene oxide; CHA: catalytic hairpin assembly; MCF7: human breast cancer cell lines; SPE: screen-printed electrode; SPCE: screen-printed carbon electrode; GO: graphene oxide; SWV: square wave voltammetry; MWCNTs: multi-walled carbon nanotubes; LNA: locked nucleic acid; p19: RNA silencing suppressor; CV: cyclic voltammetry; PNA: peptide nucleic acid; FTO: fluorine tin oxide; CGO: carboxylated graphene oxide; Au-PtBNPs: Au-Pt bimetallic nanoparticles; SA: streptavidin; CP: capture probe; Thi: thionine.

Table 1. Comparison of the analytical parameters for the most relevant miRNA-21 electrochemical biosensors reported in the last two years.